metals

MDPI

Article

Influence of the Test Configuration and Temperature on the Mechanical Behaviour of WC-Co

Luis M. González [1], Ernesto Chicardi [1], Francisco J. Gotor [2,*], Raul Bermejo [3], Luis Llanes [4] and Yadir Torres [1]

1 Department of Engineering and Materials Science and Transport, University of Seville (US), 41092 Seville, Spain; luis.gonbec@gmail.com (L.M.G.); echicardi@us.es (E.C.); ytorres@us.es (Y.T.)
2 Materials Science Institute of Seville (CSIC-US), 41092 Seville, Spain
3 Department of Materials Science, Montanuniversitaet Leoben, 8700 Leoben, Austria; raul.bermejo@unileoben.ac.at
4 Department of Materials Science and Metallurgical Engineering, Universitat Politècnica de Catalunya - BarcelonaTech, 08019 Barcelona, Spain; luis.miguel.llanes@upc.edu
* Correspondence: fgotor@cica.es; Tel.: +34-954489540

Received: 28 January 2020; Accepted: 28 February 2020; Published: 29 February 2020

Abstract: In this work, the effect of the test configuration and temperature on the mechanical behaviour of cemented carbides (WC-Co) with different carbide grain sizes (d_{WC}) and cobalt volume fractions (V_{Co}), implying different binder mean free paths (λ_{Co}), was studied. The mechanical strength was measured at 600 °C with bar-shaped specimens subjected to uniaxial four-point bending (4PB) tests and with disc specimens subjected to biaxial ball-on-three-balls (B3B) tests. The results were analysed within the frame of the Weibull theory and compared with strength measurements performed at room temperature under the same loading conditions. A mechanical degradation greater than 30% was observed when the samples were tested at 600 °C due to oxidation phenomena, but higher Weibull moduli were obtained as a result of narrower defect size distributions. A fractographic analysis was conducted with broken specimens from each test configuration. The number of fragments (N_f) and the macroscopic fracture surface were related to the flexural strength and fracture toughness of WC-Co. For a given number of fragments, higher mechanical strength values were always obtained for WC-Co grades with higher K_{Ic}. The observed differences were discussed based on a linear elastic fracture mechanics (LEFM) model, taking into account the effect of the temperature and microstructure of the cemented carbides on the mechanical strength.

Keywords: cemented carbides; temperature; mechanical strength; Weibull; biaxial test

1. Introduction

Rising competitiveness in the metal industry is driving a continuous reduction in manufacturing time and associated costs. There are many advantages of high-speed machining compared to conventional machining: higher cutting speed and amount of material eliminated in each operation, possibility of machining slimmer walls and/or hardened steel (>50 HRC, Hardness Rockwell C), more accurate contours and better dimensional tolerance, improved surface finishing with an associated reduction in polishing time, and decrease in the shaving-tool coefficient, which increases tool life. However, the service requirements for these tools are continuously increasing in terms of temperature, as well as tribological and mechanical stresses, such as impacts and cyclic loads, which often compromise the tool reliability.

Cemented carbides are widely used in cutting tools due to their excellent hardness and fracture toughness, as well as good damage tolerance under service-like conditions. However, cemented

carbides show chemical instability at high temperatures due to their poor oxidation resistance. These materials generally possess different types of natural defects with a large size distribution (pores, carbide clusters, abnormally large carbides, micro-cracks, etc.) that are associated with the fabrication process [1–3]. Moreover, other families of defects can also be generated due to the in-service operating conditions as a result of oxidation, wear, contact damage, etc. [4–6]. Therefore, cemented carbides show defect controlling fracture strength, which is associated with the size of the largest (or critical) defect in the material. This scenario leads to variability in the mechanical behaviour of the tools, and scattered values of the mechanical strength are frequently found for different specimens of the same material grade [7]. In addition, the size of the specimen and the type of test also have an important influence on the strength properties because they determine the tested volume of material and the probability of finding the critical defect [8]. For all these reasons, the strength of cemented carbides, as for other brittle materials, is primarily determined by the size distribution of critical defects, which may vary from specimen to specimen. Weibull statistical analyses are employed to estimate the probability of failure of the specimens upon applied stress. The strength is thus described as a distribution function, based on the underlying density distribution function of critical defect sizes [9]. The specimen fails if its weakest volume element fails, according to the following probability function [10]:

$$P_f(\sigma, V) = 1 - \exp\left[-\frac{V}{V_0}\left(\frac{\sigma}{\sigma_0}\right)^m\right] \quad (1)$$

where the Weibull modulus, m, describes the scatter of the strength data and the characteristic strength, σ_0, is the stress at which, for specimens of volume $V = V_0$, the failure probability is $P_f(\sigma_0,V_0) = 1 - \exp(-1) \approx 63\%$. High m values indicate small variations in fracture stress and a less volume-dependent material. In addition, the volume of material under applied tensile stress, V, influences the failure stress of the specimen. This is known as the "volume effect", and is the most important consequence of the Weibull theory. The strength of brittle materials is generally determined using standardised uniaxial three- or four-point bending test methods, which require a relatively large number of specimens with appropriate and time-consuming sample preparation, including cutting, polishing, and edge chamfering. The inadequate preparation of samples (bending bars) may introduce new defect populations in the surface to be tested, which can mask the inherent defect distribution and yield an apparent reduction in the Weibull modulus as well as in the characteristic strength of the finished product. Furthermore, measurement uncertainties associated with the experimental procedure (inaccurate positioning of the specimens, uneven contact, and transfer of load, friction, etc.) can lead to the underestimation of the Weibull parameters, which is more critical in the case of materials with relatively high Weibull moduli because these uncertainties may be in the range of the scatter of the strength values [11].

Biaxial bending tests, such as the ball-on-three balls (B3B) test [12,13], are attracting increasing interest to overcome the problem of introducing defects during sample preparation. In B3B tests, disc specimens are supported on three balls and loaded symmetrically with a fourth ball. At the midpoint of the disc surface opposite to the loading ball, a biaxial tensile stress state exists, which is used for biaxial strength testing. This method is recognised to be more tolerant of some out-of-flatness of the disc and some misalignment problems associated with the loading system, as well as edge defects related to the sample preparation process [12]. In addition, the load is transferred far away from the region of maximum stress, thus avoiding an effect on the strength. Furthermore, friction is much smaller than in the commonly used bending tests. For all these reasons, as-sintered and small specimens (real pieces) can be tested with biaxial bending methods such as the B3B [13].

In this work, the mechanical strength of three cemented carbide grades with different microstructures was determined at two temperatures (room temperature and 600 °C) using both uniaxial four-point bend (4PB) and biaxial B3B testing methods. The results were analysed using the Weibull statistical theory. The influence of the microstructure, temperature, and test configuration on the strength of the cemented carbides was investigated. Fractographic analyses were carried

out to study the sources of failure under the different test configurations and conditions. Finally, the relationship between the mechanical strength, the number of fragments, the area associated with fracture, the size of defects responsible for failure, and the fracture toughness of the different material grades were discussed in the context of the linear elastic fracture mechanics (LEFM).

2. Materials and Experimental Procedure

Three sintered cemented carbide grades (referred to as 16F, 16M, and 27C) with different combinations of carbide grain size (d_{WC}) and cobalt volume fraction (V_{Co}), implying different binder mean free paths (λ_{Co}), were studied in this work. λ_{Co} is a useful two-phase microstructural parameter that allows the comparison of cemented carbide microstructures, in which both independent variables, d_{WC} and $V_{Co,}$ vary simultaneously. They were supplied by DURIT, Metalurgia Portuguesa do Tungsténio Lda (Albergaria-a-Velha, Portugal). The microstructural parameters of each material grade, along with the Vickers hardness (HV30) and the fracture toughness (K_{Ic}) determined in previous work [14], are summarised in Table 1.

Table 1. Microstructural parameters, Vickers hardness (*HV30*), and fracture toughness (K_{Ic}) of the three cemented carbide grades [14].

Grade	V_{Co} (%)	d_{WC} (μm)	λ_{Co} (μm)	*HV30* (GPa)	K_{Ic} (MPa·m$^{1/2}$)
16F	16	0.50	0.25	15.5	9.2
16M	16	1.06	0.30	14.0	10.5
27C	27	1.66	0.76	11.2	14.7

Herein, 4PB and B3B tests were performed with a universal electro-mechanical testing machine (Model 5505, Instron Ltd., Norwood, MA, USA) at a loading rate of 100 N/s until fracture. The 4PB tests were carried out on prismatic bars with dimensions of 45 × 5 × 4 mm^3 with a fully articulated test jig using outer/inner spans of 40 mm/20 mm, 30 mm/15 mm, and 20 mm/10 mm. The B3B tests were performed on discs that were 13 mm in diameter and 1 mm in thickness with 4 alumina balls that were 3 mm in diameter. The tests were carried out at room temperature and 600 °C using molybdenum jigs in a split furnace (Energon S.L., Arganda del Rey, Spain) coupled with the testing machine (Figure 1).

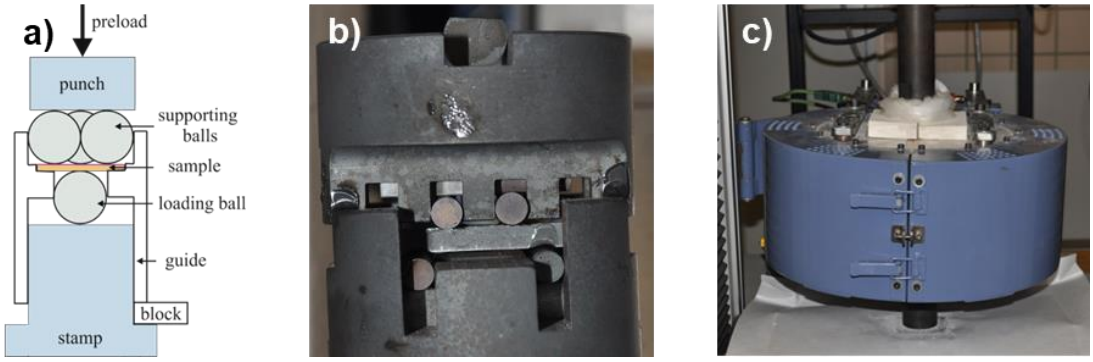

Figure 1. (**a**) Schematic of the ball-on-three-balls (B3B) testing jig; (**b**) molybdenum four-point bend (4PB) test jig; and (**c**) split furnace used for high-temperature B3B and 4PB tests.

The tensile loaded surfaces of all specimens (bars and discs) were carefully ground using diamond discs with a maximum diamond particle size of 60, 40, and 25 μm and polished with diamond powder suspensions of 9, 6, and 3 μm to avoid surface damage. Ten samples were evaluated for each grade and test condition. For the high-temperature tests, a preload of 10 N was applied at room temperature to hold the specimen to the molybdenum jig, and then the temperature was increased to approximately 600 °C at 5 °C/min, maintaining the constant preload value. A dwell time of 15 min was set at the

maximum temperature to reach thermal equilibrium, and then the test was started. The maximum stress (σ_{max}) was calculated from the maximum load at fracture for both test configurations according to the following equations [12,15]:

$$\sigma_{max,P4B} = \frac{3\,F(s_0 - s_i)}{2\,B\,h^2} \quad (2)$$

$$\sigma_{max,B3B} = f \cdot \frac{F}{t_2} \quad (3)$$

where F is the applied load at fracture; s_0 and s_i are the outer and inner spans, respectively; B and h are the width and height of the bar specimen, respectively; t is the thickness of the disc specimen; and f is a dimensionless factor (calculated from reference [16]), which depends on the geometry of the specimen and the balls, the Poisson's ratio of the tested material, and the load transfer from the jig into the specimen [12].

After mechanical testing, a fractographic examination of selected specimens was conducted via scanning electron microscopy (SEM) (S-4800 SEM-FEG, Hitachi High-Tech, Fukuoka, Japan) to discern the origin and size of the strength-limiting defects. The total surface area of the fracture (S_f), the micromechanisms associated with the fracture and the number of fragments (N_f) for the different testing conditions were also analysed.

3. Results and Discussion

Figure 2 shows the Weibull diagrams for the three cemented carbide grades subjected to B3B and 4PB tests at room temperature and 600 °C. The values of the Weibull parameters, m and σ_0 (with a 90% confidence interval), are included in Table 2 for each grade, temperature, and test configuration. These values were calculated in accordance with the standard EN-843-5 [17] as follows:

$$\ln\ln\left(\frac{1}{1-P_f}\right) = m \cdot \ln\sigma - m \cdot \ln\sigma_0 \quad (4)$$

The broken lines in Figure 2 represent the best fit of the strength data according to Equation (4) using the maximum likelihood method. The 90% confidence interval for the measured values represents the range where the true Weibull parameters (from the parent distribution) can be found with a 90% probability and reflects the influence of the sampling procedure. These figures show that, in most cases, the failure stress values follow a Weibull distribution associated with the defect size distribution in the specimens.

However, in Figure 2, a deviation from the Weibull distributed strength was observed in the 16M and 27C grades, especially for the B3B tests performed at room temperature, in which a "banana-shape" strength distribution was observed. This behaviour suggests the existence of a kind of threshold strength value at approximately 2800 MPa. When using the B3B test, the region under high flexural stress is reduced compared to the 4PB test, and this region can be smaller than the size of the larger defects in the samples. Therefore, the failure associated with such defects might not take place during the test. Nevertheless, this behaviour can also be explained if the defects in the material are never larger than a certain critical size.

Moreover, as a general rule, higher failure stress values and, therefore, higher characteristic strength values were obtained from the B3B tests than from the 4PB tests. This fact can be explained according to the "volume effect" in Weibull theory, i.e., the probability of containing larger defects (failure) increases as the size of the tested specimen increases [10]. In the biaxial configuration, there is a lower effective volume (or effective surface) of material tested, and as a result, higher strength values are expected. If some large flaws are located in a low flexural stress region, these defects will not cause fracture. In the B3B tests, more than 90% of the maximal stress is located in the central region between the three balls (1/20th of the specimen dimension), which is much smaller than the region under the maximal stress in the 4PB tests located between the inner spans. Only small differences in

strength were obtained between the 4PB tests performed using different spans, although this same trend was observed, as shown in Table 2. In a previous paper [9], an effective volume of ~10 mm^3 and ~5 mm^3 was estimated for P4B specimens with 40–20 mm and 20–10 mm spans, respectively, whereas a significantly lower effective volume ranging from 0.005 to 0.03 mm^3 was calculated for the B3B specimens depending on the disc thickness.

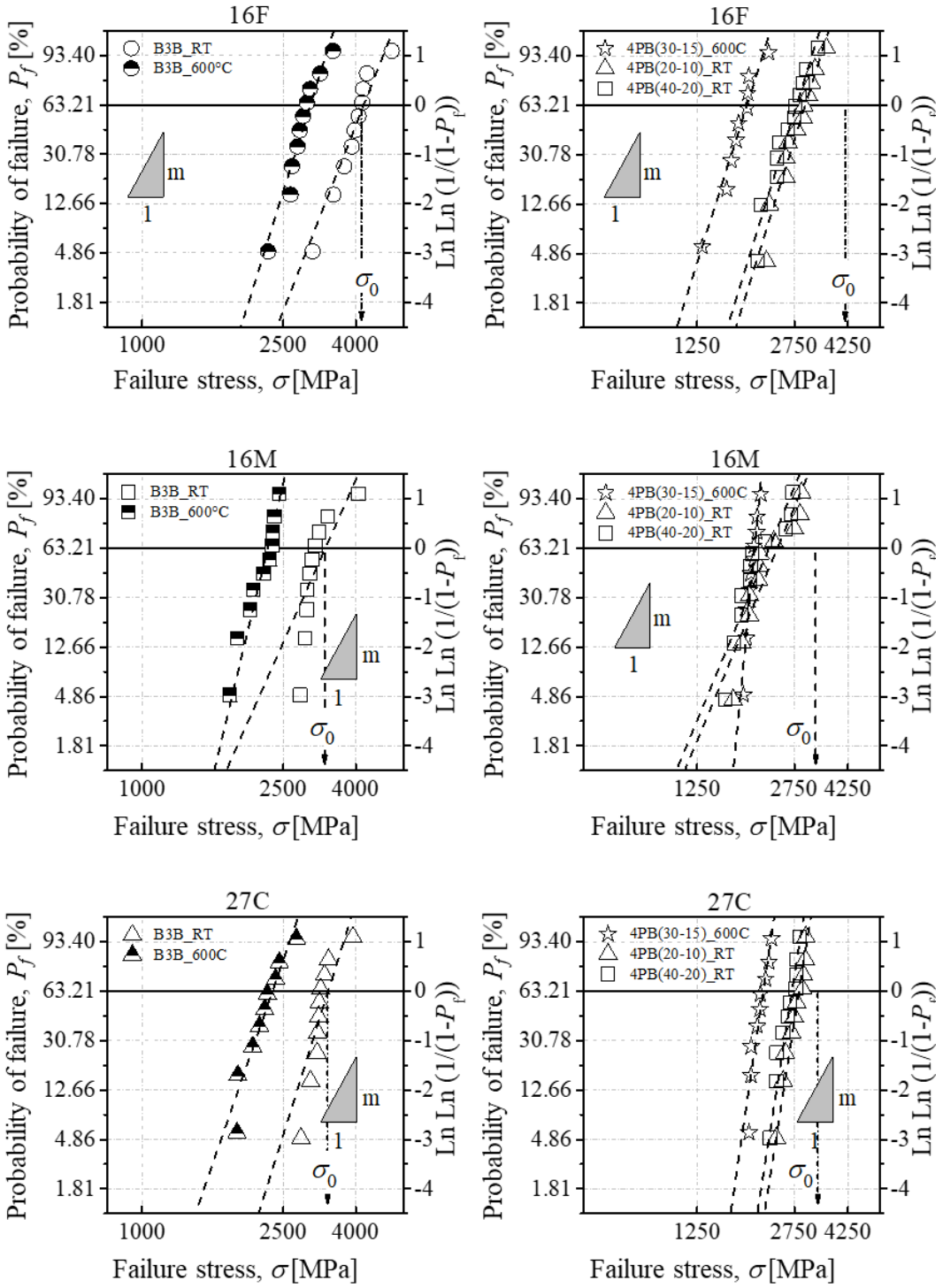

Figure 2. Weibull diagrams of the three cemented carbide grades subjected to B3B and 4PB tests at room temperature and 600 °C.

Table 2. Weibull parameters estimated under B3B and P4B tests for the three cemented carbide grades (16F, 16M, and 27C) at room temperature (RT) and 600 °C.

Grade	$\sigma_0 \times 10^3$ (MPa)					m				
	B3B		4PB			B3B		4PB		
			(20–10)	(40–20)	(30–15)			(20–10)	(40–20)	(30–15)
	RT	600 °C	RT	RT	600 °C	RT	600 °C	RT	RT	600 °C
16F	4.2 (3.9–4.6)	3.0 (2.8–3.2)	3.0 (2.8–3.2)	2.8 (2.6–3.0)	1.8 (1.7–2.0)	8 (4–11)	10 (5–13)	8 (5–11)	8 (4–11)	8 (4–11)
16M	3.3 (3.0–3.6)	2.3 (2.2–2.4)	2.4 (2.2-2.7)	2.2 (2.0–2.5)	2.0 (1.9–2.1)	7 (4–10)	13 (7–17)	6 (3–7)	6 (3–8)	26 (14–35)
27C	3.3 (3.1–3.6)	2.3 (2.2–2.5)	2.9 (2.7–3.0)	2.7 (2.6–2.8)	2.1 (2.0–2.2)	10 (6–13)	9 (5–12)	16 (9–22)	16 (9–21)	17 (9–24)

From Figure 2, the influence of the microstructure of the cemented carbide grades, especially λ_{Co}, on the mechanical strength for both temperatures and test configurations can be extracted. Regardless of the temperature, the B3B tests seem to be more sensitive to the microstructure and size of critical defects. Differences between cemented carbide grades are higher in the B3B tests than in the 4PB tests. B3B tests showed that the 16F grade, which has the lowest λ_{Co} value, possessed the highest mechanical strength regardless of the temperature. However, the mechanical strength at 600 °C obtained from the 4PB tests did not show significant differences for the different cemented carbide grades. The 16M and 27C grades exhibited similar failure stresses in the B3B tests at both room and elevated temperatures. Likewise, the 16F and 27C grades exhibited similar mechanical strength values at both temperatures, when tested under 4PB. For the 4PB test configuration, the 16M grade exhibited the lowest strength at room temperature. In general, for both test configurations and temperatures, highest mechanical strength was observed for the 16F grade (lowest λ_{Co}) as a result of a greater constraint degree exerted by the carbide phase on the binder.

The results in Figure 2 and Table 2 clearly show an important strength degradation just after 15 min at 600 °C, which was certainly due to incipient oxidation on the specimen surface that produced larger critical defects. Although oxidation phenomena have been observed in cemented carbides at temperatures as low as 500 °C [18], the degradation in the mechanical properties begins to become significant just above 600 °C [19]. For example, a strong reduction in the room-temperature mechanical strength has been reported after short exposure times in air at 700 °C (10–60 min) [20]. The extent of this degradation depends, of course, on the temperature, but other factors can also be involved, such as the binder content, the carbide grain size, the oxidising atmosphere (oxygen content) and/or the high-temperature exposure time [18]. It has been postulated that the reduction in the mechanical strength is associated with the formation of oxidation products (WO_3 and $CoWO_4$) and the development of new microstructural defects [19,20].

From the B3B tests, an approximately 30% reduction in strength was observed for the three grades. However, for 4PB tests, different levels of degradation were evidenced; the 16F grade (lowest λ_{Co}) exhibited the highest degradation, whereas the 16M grade, which exhibited the lowest mechanical strength at room temperature, had the lowest degradation. The different behaviour between both tests may be, again, a consequence of the defect size distribution in the samples and the different effective volumes tested. Note from Figure 2 that the Weibull diagrams of the 4PB tests for the different grades at room temperature tend to diverge at lower failure stress values (larger defects), whereas at higher stress values (smaller defects), the differences are significantly reduced and, in some cases, negligible. However, at 600 °C, the differences between the Weibull diagrams of the three grades are significantly reduced in a wider range of the failure stress, suggesting that, due to oxidation, the size distribution of defects became more homogeneous and similar for all the samples.

The homogenisation of the defect size distribution at high temperatures also increases the Weibull modulus. Oxidation not only created larger defects but also with a more homogenous size than those associated with processing. The Weibull modulus values in Table 2 allow the extraction of additional considerations related to the influence of the microstructure of cemented carbide grades. If the 16F and 16M grades are compared (same binder content but different carbide size), a higher Weibull modulus, which implies a narrower defect size distribution, was obtained at 600 °C for the grade with a larger carbide size (16M). Nevertheless, the size of the critical defects for the 16F grade remained smaller, as observed at room temperature (higher characteristic strength). This behaviour can be explained by the fact that larger WC grains have a greater tendency to be oxidised, generating larger, although more homogeneous, defects.

However, for the 27C grade, with a higher binder content and larger carbide grains, the Weibull modulus remained practically unchanged at 600 °C, although the characteristic strength was reduced. This finding means that the defects were larger than those at room temperature but with a similar size distribution, i.e., the defect size distribution was just shifted to larger size values. Note that the 27C grade possessed the largest Weibull modulus at room temperature. It can be speculated that the intrinsic defects associated with processing may have experienced subcritical crack growth, associated with R-curve behaviour. This behaviour can also be the result of a lower oxidation extent for this material grade, which is in agreement with the results reported by Basu and Sarin [18], in which higher oxidation was observed in WC-Co as the Co content was reduced.

Finally, Figure 2 also indicates that regardless of the test temperature, the influence of the test configuration is less important when the content of the binder phase is increased because the material has a higher damage tolerance. This fact is more clearly observed at 600 °C, where the defect size distribution becomes more homogeneous, in such a way that the differences were reduced between the largest flaw populations that induced failure in the highly stressed region corresponding to each test configuration.

Figure 3 shows the relationship between the number of fragments generated due to the fracture process (N_f) and the mechanical strength (σ) for the three WC-Co grades evaluated at both temperatures and test configurations, from which a direct correlation between both parameters can be extracted. In general, a higher number of fragments was obtained when the mechanical strength of the specimens increased. This direct correlation between N_f and σ is the result of the excess strain energy stored in the material during bending, which is released at fracture. In specimens with the highest mechanical strengths, the broken pieces generated were so numerous that some of them were impossible to collect, which caused N_f scattered values. For the three grades and the B3B configuration, the number of fragments of the tested samples was always smaller at 600 °C due to the presence of larger and more homogeneous defects. This behaviour was not observed so clearly in the samples tested under the 4PB configuration, except for the 16F grade, which exhibited, as mentioned above, the largest mechanical degradation at 600 °C. Moreover, N_f also correlates with K_{Ic}. In this sense, if the 16M and 27C grades with similar strength are compared, the differences found in N_f are associated in this case with the different K_{Ic} values between both grades.

The correlation between σ, K_{Ic}, and the total fracture surface area (S_f) (or N_f) can be expressed by the following equation, which was derived theoretically by considering the microscopic and macroscopic energy balance in the propagation of the crack causing the fracture of the test piece [21]:

$$\sigma = \phi \, K_{Ic} \, S_f^{1/2} \tag{5}$$

where the parameter ϕ is a shape factor, which depends on the material and geometry and was set to 1.1. Equation (5) states that, at a given S_f (or N_f), there is a direct correlation between σ and K_{Ic}; σ will be higher for a specimen with higher K_{Ic}. This dependence can be used to qualitatively compare the resistance to crack propagation between grades based on the number of broken pieces generated in a bending test.

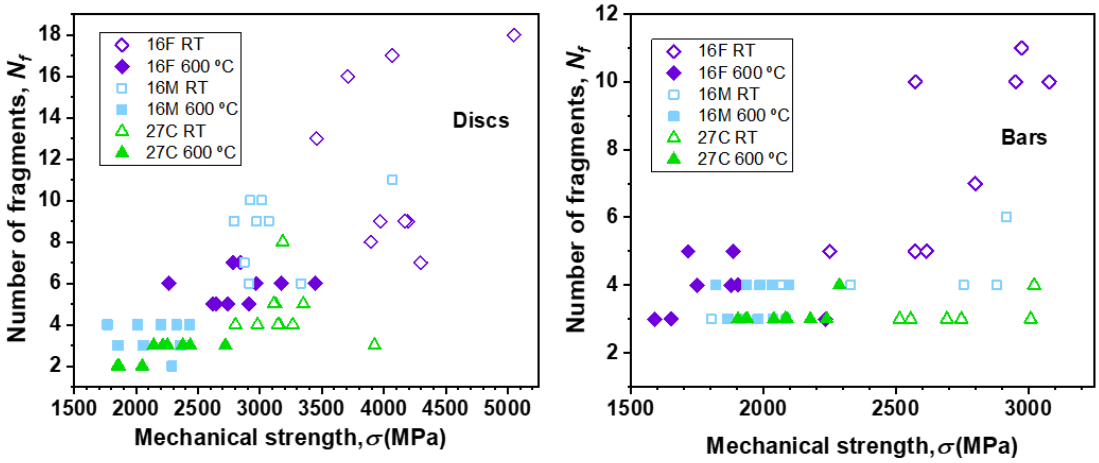

Figure 3. Relationship between the number of fragments (N_f) in the broken samples from the B3B and 4PB tests and the mechanical strength (σ).

In Figure 4, σ is plotted versus $S_f^{1/2}$ for some representative bar specimens of the three cemented carbide grades. The results obtained for Si_3N_4-based ceramics and 10 wt.% WC-Co are also included in Figure 4 [21,22]. A linear correlation was observed, which is in agreement with Equation (5). According to this same equation, the ratio between the slopes of the linear fit corresponding to two different materials should allow the estimation of the ratio between their fracture toughness values (if ø is equal for both materials). In this sense, from the slopes of the 16M and 27C grades in Figure 4, a ratio of 0.9 was obtained, which was close to the value of 0.71 obtained for the ratio of K_{Ic} values for these two grades measured by the single edge notched bend (SENB) method [14].

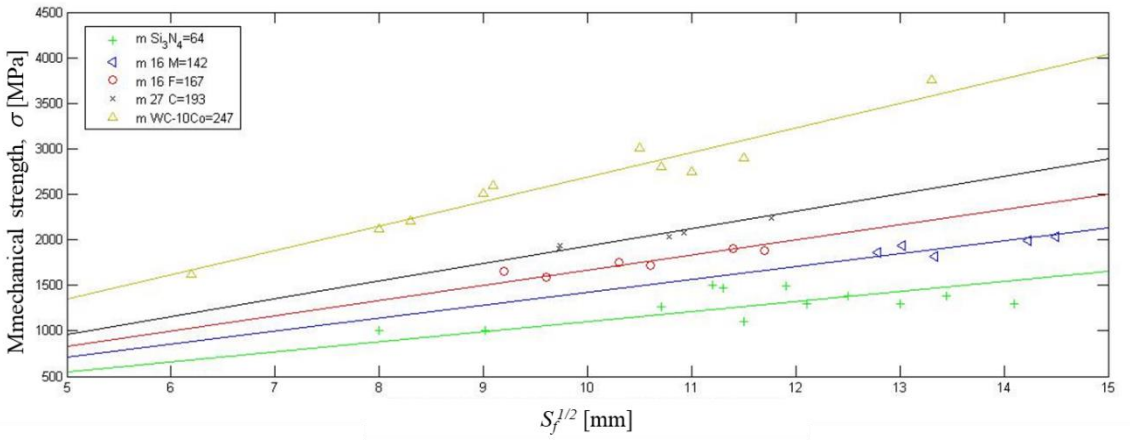

Figure 4. Relationship between the mechanical strength (σ) and the square root of the total fracture surface area ($S_f^{1/2}$) for specimens subjected to P4B tests. Note that the results for two new materials are included from references [21,22].

A fractographic analysis was also performed, and Figure 5 shows representative SEM micrographs of the fracture surfaces of the three cemented carbide grades at room temperature and 600 °C, where the characteristic critical defects (marked with squares) can be observed. In the images at low magnification (Figure 5c,e), the typical radial marks or ridges emanating from the origin of the fracture are easily seen. Failure was always initiated at or near the surface subjected to the maximum stress. Typical processing flaws, such as pores, large carbide grains, or agglomerates without cobalt, were generally found.

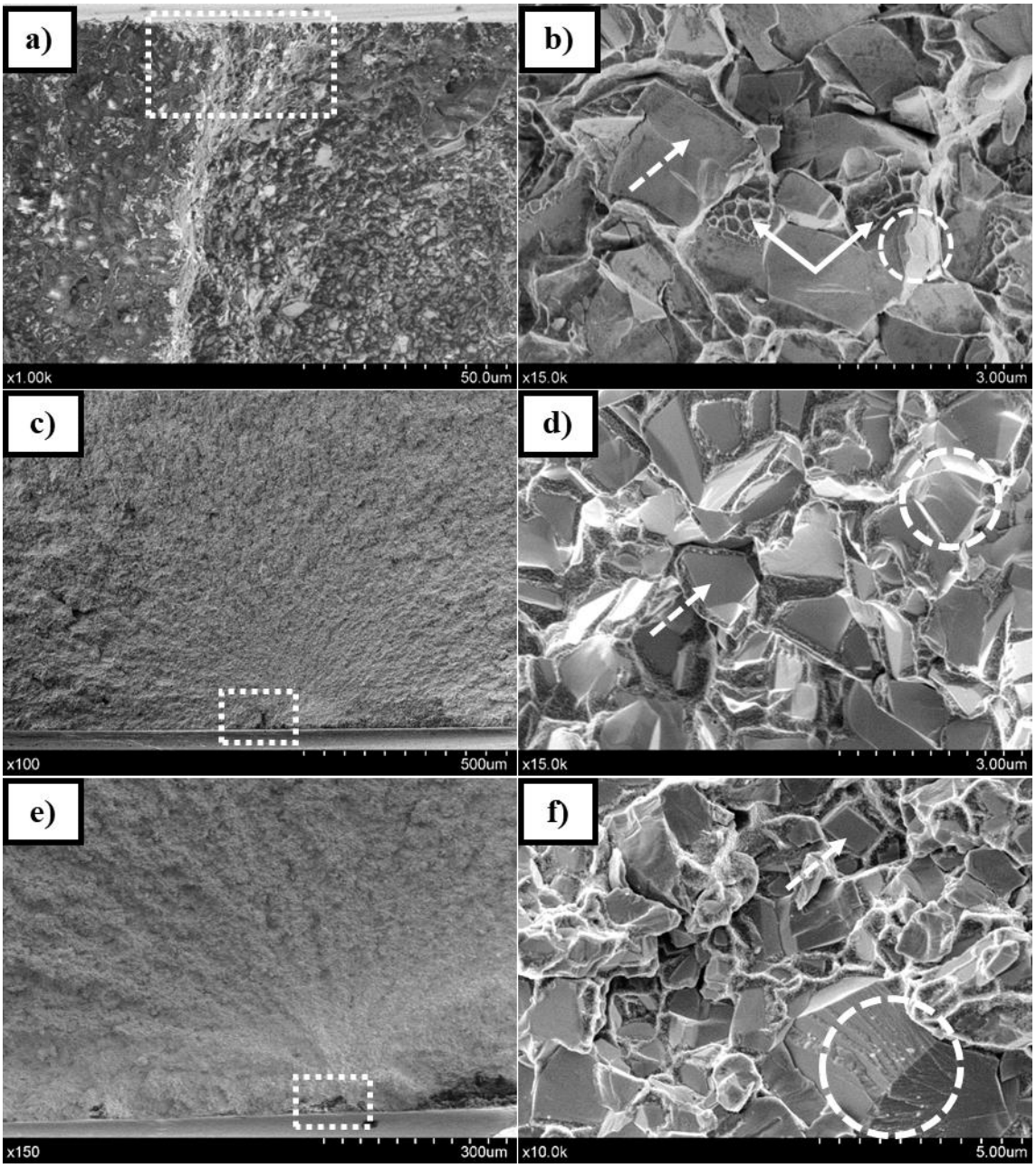

Figure 5. Representative SEM micrographs of the fracture surfaces showing the fracture origin (dotted squares) and the unstable fracture region, where the micromechanisms associated to the fracture are shown: dimples (straight arrows), cleavage (dotted arrows), and river patterns (dotted circles). (**a**,**b**) The 27C grade at room temperature, (**c**,**d**) the 16M grade at 600 °C, and (**e**,**f**) the 27C grade at 600 °C.

Details of the micromechanisms responsible for the fracture in the cemented carbides during the flexural tests at RT and 600 °C are also shown in Figure 5b,d,f. A transgranular fracture was always observed. The presence of carbide cleavages (marked with dotted arrows in the figure) and river patterns (marked with dotted circles in figure), characteristics of brittle materials, was evidenced. The presence of dimples (marked with straight arrows in the figure) associated with ductile fracture was more clearly detected in specimens tested at room temperature. At 600 °C, oxidation was especially observed in the binder phase, which appears with a pseudo-granular aspect (Figure 5d,f).

The formation of oxidation products with a more brittle nature that replace the former ductile binder phase plays a key role in the degradation of the mechanical strength [23].

The fracture toughness of the different cemented carbide grades was estimated under the frame of the LEFM approach from the fracture surface area and Equation (5) and from the critical defect size (a_c) causing the failure [24], using the following equation [25]:

$$K_{Ic} = Y\,\sigma\,(\pi a_c)^{1/2} \quad (6)$$

where Y is a dimensionless geometric factor depending on the geometry and location of the defect and on the loading configuration. Y is approximately equal to $2/\pi$ if the failure-controlling defect is a circular flaw located underneath the tensile surface, as generally found in the specimens tested at room temperature. However, for flaws reaching out of the surface, as observed in the specimens tested at 600 °C, the Y factor should be chosen as $\sim(2/\pi)\cdot 2^{1/2}$, which implies that they are more critical than subsurface flaws.

The K_{Ic} values for the three cemented carbide grades estimated from these two methods are listed in Table 3 and are compared with experimental ones evaluated by SENB [14]. In general, there is a good correlation between the different values obtained, although higher differences were observed when K_{Ic} was estimated in samples tested under the B3B configuration. These differences are related to the difficulties in discerning and measuring the critical defects originating the fracture in small samples that have also stored a substantial amount of energy during bending and breaking into many small fragments.

Table 3. Fracture toughness estimated from the fracture surface area (Equation (5)) and the critical defect size (Equation (6)) for three cemented carbide grades compared with experimental results obtained by single edge notched bend (SENB).

Grade	Measured K_{Ic} by SENB at RT [14] (MPam$^{1/2}$)	Discs		Bars	
		Estimated K_{Ic} from Equation (5) (MPam$^{1/2}$)	Estimated K_{Ic} from Equation (6) (MPam$^{1/2}$)	Estimated K_{Ic} from Equation (5) (MPam$^{1/2}$)	Estimated K_{Ic} from Equation (6) (MPam$^{1/2}$)
16F	9.2	10.3	*	9.4	8.0
16M	10.5	9.5	10.3	9.6	14.9
27C	14.7	10.5	12.5	13.5	17.9

* Unable to measure the defect size that originated the fracture.

4. Conclusions

The effect of temperature on the strength distribution of three WC-Co grades with different binder mean free paths (named 16F, 16M, and 27C) has been demonstrated using uniaxial and biaxial bending tests between RT and 600 °C. A higher characteristic strength was obtained in biaxial bending as a consequence of a size effect. The influence of microstructure on the strength distribution was more evident by using the B3B test for both room and elevated temperatures. A mechanical degradation greater than 30% was observed when the samples were tested at 600 °C due to oxidation phenomena. However, higher Weibull moduli were obtained as a result of narrower defect size distributions. A direct correlation between the number of fragments due to fracture (or the total fracture surface area) and the mechanical strength was observed. For a given number of fragments, higher mechanical strength values were always obtained for grades with higher K_{Ic}. The existence of surface defects was confirmed by fractography, and the validity of using biaxial testing was demonstrated at room and elevated temperatures, which is of special interest for evaluating the mechanical strength of small samples.

Author Contributions: The authors of this work have contributed in all steps, from the conceptualization of the research idea to the final writing. All authors have read and agreed to the published version of the manuscript.

Funding: This research was funded by the Junta de Andalucía under grant number P12-TEP-2622.

Acknowledgments: The authors want to thank the laboratory technicians Jesus Pinto and Mercedes Sánchez for their assistance with mechanical testing.

Conflicts of Interest: The authors declare no conflict of interest.

References

1. Davidge, R.W. *Mechanical Behaviour of Ceramics*; Cambridge University Press: London, UK, 1979.
2. Danzer, R. Ceramics: Mechanical performance and lifetime prediction. In *Encyclopedia of Advanced Materials*; Cahn, R.W., Brook, R., Eds.; Pergamon Press: Oxford, UK, 1994; pp. 385–398.
3. Munz, D.; Fett, T. *Ceramics: Mechanical Properties, Failure Behaviour, Materials Selection*; Springer: Berlin, Germany, 1999.
4. Kotas, A.B.; Danninger, H.; Weiss, B.; Mingard, K.; Sanchez, J.; Llanes, L. Fatigue testing and properties of hardmetals in the gigacycle range. *Int. J. Refract. Met. Hard Mater.* **2017**, *62*, 183–191. [CrossRef]
5. Huang, S.; Xiong, J.; Guo, Z.; Wan, W.; Tang, L.; Zhong, H.; Zhou, W.; Wang, B. Oxidation of WC-TiC-TaC-Co hard materials at relatively low temperature. *Int. J. Refract. Met. Hard Mater.* **2015**, *48*, 134–140. [CrossRef]
6. Krobath, M.; Klunsner, T.; Ecker, W.; Deller, M.; Leitner, N.; Marsoner, S. Tensile stresses in fine blanking tools and their relevance to tool fracture behaviour. *Int. J. Mach. Tools Manuf.* **2018**, *126*, 44–50. [CrossRef]
7. Danzer, R.; Lube, T.; Supancic, P.; Damani, R. Fracture of ceramics. *Adv. Eng. Mater.* **2008**, *10*, 275–298. [CrossRef]
8. Jonke, M.; Klünsner, T.; Supancic, P.; Harrer, W.; Glätzle, J.; Barbist, R.; Ebner, R. Strength of WC-Co hard metals as a function of the effectively loaded volume. *Int. J. Refract. Met. Hard Mater.* **2017**, *64*, 219–224. [CrossRef]
9. Torres, Y.; Bermejo, R.; Gotor, F.J.; Chicardi, E.; Llanes, L. Analysis on the mechanical strength of WC-Co cemented carbides under uniaxial and biaxial bending. *Mater. Des.* **2014**, *55*, 851–856. [CrossRef]
10. Weibull, W. A statistical distribution function of wide applicability. *J. Appl. Mech.* **1951**, *18*, 293–297.
11. Bermejo, R.; Supancic, P.; Danzer, R. Influence of measurement uncertainties on the determination of the Weibull distribution. *J. Eur. Ceram. Soc.* **2012**, *32*, 251–255. [CrossRef]
12. Börger, A.; Supancic, P.; Danzer, R. The ball on three balls test for strength testing of brittle discs: Stress distribution in the disc. *J. Eur. Ceram. Soc.* **2002**, *22*, 1425–1436. [CrossRef]
13. Danzer, R.; Harrer, W.; Supancic, P.; Lube, T.; Wang, Z.; Börger, A. The ball on three balls test—Strength and failure analysis of different materials. *J. Eur. Ceram. Soc.* **2007**, *27*, 1481–1485. [CrossRef]
14. Llanes, L.; Torres, Y.; Anglada, M. On the fatigue crack growth behavior of WC–Co cemented carbides: Kinetics description, microstructural effects and fatigue sensitivity. *Acta Mater.* **2002**, *50*, 2381–2393. [CrossRef]
15. EN 843-1. In *Advanced Technical Ceramics, Monolithic Ceramics, Mechanical Properties at Room Temperature, Part 1: Determination of Flexural Strength*; European Committee for Standardization: Brussels, Belgium, 1995.
16. Ball-on-3-Balls Test (B3B)—Strength Testing. Available online: http://www.isfk.at/de/960/ (accessed on 2 December 2013).
17. EN 843-5. In *Advanced Technical Ceramics, Monolithic Ceramics, Mechanical Properties at Room Temperature, Part 5: Statistical Analysis*; European Committee for Standardization: Brussels, Belgium, 1997.
18. Basu, S.; Sarin, V. Oxidation behavior of WC-Co. *Mater. Sci. Eng. A* **1996**, *209*, 206–212. [CrossRef]
19. Acchar, W.; Gomes, U.; Kaysser, W.; Goring, J. Strength degradation of a tungsten carbide-cobalt composite at elevated temperatures. *Mater. Charact.* **1999**, *43*, 27–32. [CrossRef]
20. Casas, B.; Ramis, X.; Anglada, M.; Salla, J.M.; Llanes, L. Oxidation-induced strength degradation of WC–Co hardmetals. *Int. J. Refract. Met. Hard Mater.* **2001**, *19*, 303–309. [CrossRef]
21. Yanaba, Y.; Hayashi, K. Relation between fracture surface area of a flexural strength specimen and fracture toughness for WC-10mass%Co cemented carbide and Si_3N_4 ceramics. *Mater. Sci. Eng. A* **1996**, *209*, 169–174. [CrossRef]
22. Torres, Y.; Casellas, D.; Anglada, M.; Llanes, L. Fracture toughness evaluation of hardmetals: Influence of testing procedure. *Int. J. Refract. Met. Hard Mater.* **2001**, *19*, 27–34. [CrossRef]
23. Chicardi, E.; Bermejo, R.; Gotor, F.J.; Llanes, L.; Torres, Y. Influence of temperature on the biaxial strength of cemented carbides with different microstructures. *Int. J. Refract. Met. Hard Mater.* **2018**, *71*, 82–91. [CrossRef]

24. Munro, R.G.; Freiman, S.W. Correlation of fracture toughness and strength. *J. Am. Ceram. Soc.* **1999**, *82*, 2246–2248. [CrossRef]
25. Griffith, A.A. The phenomenon of rupture and flow in solids. *Philos. Trans. R. Soc. London* **1920**, *A221*, 163–198.